

PREPARED FOR SUBMISSION TO JCAP

# Updated Collider and Direct Detection Constraints on Dark Matter Models for the Galactic Center Gamma-Ray Excess

Miguel Escudero,<sup>a,b</sup> Dan Hooper<sup>b,c,d</sup> and Samuel J. Witte<sup>b,e</sup>

<sup>a</sup>Instituto de Física Corpuscular (IFIC), CSIC-Universitat de València, Apartado de Correos 22085, E-46071 Valencia, Spain

<sup>b</sup>Fermi National Accelerator Laboratory, Center for Particle Astrophysics, Batavia, IL 60510

<sup>c</sup>University of Chicago, Department of Astronomy and Astrophysics, Chicago, IL 60637

<sup>d</sup>University of Chicago, Kavli Institute for Cosmological Physics, Chicago, IL 60637

<sup>e</sup>University of California, Los Angeles, Department of Physics and Astronomy, Los Angeles, CA 90095

E-mail: [miguel.escudero@ific.uv.es](mailto:miguel.escudero@ific.uv.es), [dhooper@fnal.gov](mailto:dhooper@fnal.gov), [switte@physics.ucla.edu](mailto:switte@physics.ucla.edu)

**Abstract.** Utilizing an exhaustive set of simplified models, we revisit dark matter scenarios potentially capable of generating the observed Galactic Center gamma-ray excess, updating constraints from the LUX and PandaX-II experiments, as well as from the LHC and other colliders. We identify a variety of pseudoscalar mediated models that remain consistent with all constraints. In contrast, dark matter candidates which annihilate through a spin-1 mediator are ruled out by direct detection constraints unless the mass of the mediator is near an annihilation resonance, or the mediator has a purely vector coupling to the dark matter and a purely axial coupling to Standard Model fermions. All scenarios in which the dark matter annihilates through  $t$ -channel processes are now ruled out by a combination of the constraints from LUX/PandaX-II and the LHC.

---

<sup>1</sup>ORCID: <http://orcid.org/0000-0002-4487-8742>

<sup>2</sup>ORCID: <http://orcid.org/0000-0001-8837-4127>

<sup>3</sup>ORCID: <http://orcid.org/0000-0003-4649-3085>

---

## Contents

<b>1</b>	<b>Introduction</b>	<b>1</b>
<b>2</b>	<b>Constraints</b>	<b>3</b>
2.1	LHC	3
2.2	LEP-II	4
2.3	BaBar	4
2.4	Direct Detection	4
<b>3</b>	<b>Pseudoscalar Mediated Dark Matter</b>	<b>5</b>
<b>4</b>	<b>Vector Mediated Dark Matter</b>	<b>9</b>
<b>5</b>	<b>Dark Matter Annihilating Through <math>t</math>-Channel Mediators</b>	<b>12</b>
<b>6</b>	<b>Summary and Conclusions</b>	<b>13</b>

---

## 1 Introduction

Over the past decade or so, a number of observations have been interpreted as possible signals of annihilating or decaying dark matter particles. Examples of such observations include the 511 keV emission from the Galactic Bulge [1], an excess of synchrotron emission known as the WMAP Haze [2, 3], an excess of high energy positrons in the cosmic ray spectrum [4, 5], a mono-energetic line of 130 GeV gamma rays from the Galactic Halo [6], and a 3.5 keV X-ray line from Perseus and other galaxy clusters [7, 8]. Each of these anomalies, however, has either failed to be confirmed by subsequent measurements [9, 10], or has been shown to be quite plausibly explained by astrophysical phenomena [11–14].

In comparison to these other anomalous signals, the gamma-ray excess observed from the Galactic Center by the Fermi Gamma-Ray Space Telescope stands out. This signal has been studied in detail over the past seven years [15–25] and has been shown with high statistical significance to exhibit a spectrum, morphology and overall intensity that is compatible with that predicted from annihilating dark matter particles in the form of a  $\sim 30$ -70 GeV thermal relic distributed with a profile similar to that favored by numerical simulations. Although astrophysical interpretations of this signal have been proposed (consisting of either a large population of millisecond pulsars [26–33], or a series of recent leptonic cosmic-ray outbursts [34–36]), these explanations require either a significant degree of tuning in their parameters [34], or pulsar populations which are very different from those observed in the environments of globular clusters or in the field of the Milky Way [26, 31, 32]. In addition, some modest support for a dark matter interpretation of this signal has recently appeared in the form of excesses in the cosmic-ray antiproton spectrum [37–39], in the gamma-ray emission from the dwarf spheroidal galaxies Reticulum II and Tucana III [40–44], and from the observation of spatially extended gamma-ray emission from two dark matter subhalo candidates [45–48]. At this point in time, however, there is no clear resolution to the question of the origin of the Galactic Center excess.

<i>Dark Matter</i>	<i>Mediator</i>	<i>Interactions</i>	<i>Direct Detection</i>
Dirac Fermion, $\chi$	Spin-0	$\bar{\chi}\gamma^5\chi, \bar{f}f$	$\sigma_{\text{SI}} \propto (q/2m_\chi)^2$
Majorana Fermion, $\chi$	Spin-0	$\bar{\chi}\gamma^5\chi, \bar{f}f$	$\sigma_{\text{SI}} \propto (q/2m_\chi)^2$
Dirac Fermion, $\chi$	Spin-0	$\bar{\chi}\gamma^5\chi, \bar{f}\gamma^5f$	$\sigma_{\text{SD}} \propto (q^2/4m_n m_\chi)^2$
Majorana Fermion, $\chi$	Spin-0	$\bar{\chi}\gamma^5\chi, \bar{f}\gamma^5f$	$\sigma_{\text{SD}} \propto (q^2/4m_n m_\chi)^2$
Complex Scalar, $\phi$	Spin-0	$\phi^\dagger\phi, \bar{f}\gamma^5f$	$\sigma_{\text{SD}} \propto (q/2m_n)^2$
Real Scalar, $\phi$	Spin-0	$\phi^2, \bar{f}\gamma^5f$	$\sigma_{\text{SD}} \propto (q/2m_n)^2$
Complex Vector, $X$	Spin-0	$X_\mu^\dagger X^\mu, \bar{f}\gamma^5f$	$\sigma_{\text{SD}} \propto (q/2m_n)^2$
Real Vector, $X$	Spin-0	$X_\mu X^\mu, \bar{f}\gamma^5f$	$\sigma_{\text{SD}} \propto (q/2m_n)^2$
Dirac Fermion, $\chi$	Spin-1	$\bar{\chi}\gamma^\mu\chi, \bar{b}\gamma_\mu b$	$\sigma_{\text{SI}} \sim \text{loop (vector)}$
Dirac Fermion, $\chi$	Spin-1	$\bar{\chi}\gamma^\mu\chi, \bar{f}\gamma_\mu\gamma^5f$	$\sigma_{\text{SD}} \propto (q/2m_n)^2$ or $(q/2m_\chi)^2$
Dirac Fermion, $\chi$	Spin-1	$\bar{\chi}\gamma^\mu\gamma^5\chi, \bar{f}\gamma_\mu\gamma^5f$	$\sigma_{\text{SD}} \sim 1$
Majorana Fermion, $\chi$	Spin-1	$\bar{\chi}\gamma^\mu\gamma^5\chi, \bar{f}\gamma_\mu\gamma^5f$	$\sigma_{\text{SD}} \sim 1$
Dirac Fermion, $\chi$	Spin-0 ( <i>t</i> -ch.)	$\bar{\chi}(1 \pm \gamma^5)b$	$\sigma_{\text{SI}} \propto \text{loop (vector)}$
Dirac Fermion, $\chi$	Spin-1 ( <i>t</i> -ch.)	$\bar{\chi}\gamma^\mu(1 \pm \gamma^5)b$	$\sigma_{\text{SI}} \propto \text{loop (vector)}$
Complex Vector, $X$	Spin-1/2 ( <i>t</i> -ch.)	$X_\mu^\dagger\gamma^\mu(1 \pm \gamma^5)b$	$\sigma_{\text{SI}} \propto \text{loop (vector)}$
Real Vector, $X$	Spin-1/2 ( <i>t</i> -ch.)	$X_\mu\gamma^\mu(1 \pm \gamma^5)b$	$\sigma_{\text{SI}} \propto \text{loop (vector)}$

**Table 1.** A summary of the simplified models identified in Ref. [49] as being potentially capable of generating the observed characteristics of the Galactic Center gamma-ray excess without violating collider or direct detection constraints (as of June 2014). For each model, we list the nature of the dark matter candidate and the mediator, as well as the form of the mediator’s interactions. In the final column, we list whether the leading elastic scattering cross section with nuclei is spin-independent (SI) or spin-dependent (SD) and whether it is suppressed by powers of momentum,  $q$ , or by loops.

Many groups have studied dark matter models that are capable of generating the observed features of the Galactic Center excess (for an incomplete list, see Refs. [49–67]). In this study, we follow an approach similar to that taken in Ref. [49], and consider an exhaustive list of simplified models that are capable of generating the observed gamma-ray excess while remaining consistent with all constraints from collider and direct detection experiments. Also following Ref. [49], we choose to not consider hidden sector models in this study, in which the dark matter annihilates to unstable particles which reside in the hidden sector, without sizable couplings to the Standard Model (SM) [59, 62, 63]. While such scenarios certainly remain viable, we consider them to be beyond the scope of this work.

The models found in Ref. [49] to be compatible with existing constraints from direct detection and collider experiments are listed in Table 1, and can be divided into three categories. First, there are models in which the dark matter annihilates into SM quarks through the  $s$ -channel exchange of a spin-zero mediator with pseudoscalar couplings. These models allow for an unsuppressed ( $s$ -wave) low-velocity annihilation cross section while generating a cross section for elastic scattering with nuclei that is suppressed by either two or four powers of momentum, thus evading direct detection constraints. In the second class of models, the dark matter annihilates through the  $s$ -channel exchange of a vector boson. In this case, it was found that direct detection constraints could be evaded if the mediator couples axially with

quarks or couples only to the third generation. Lastly, there are models in which the dark matter annihilates to  $b$ -quarks through the  $t$ -channel exchange of a colored and electrically charged mediator.

In this paper, we revisit this collection of dark matter models, applying updated constraints from the Large Hadron Collider (LHC) and other collider experiments, in addition to recent constraints from the direct detection experiments LUX [68] and PandaX-II [69]. We find that many of the models previously considered within the context of the Galactic Center excess are now excluded by a combination of these constraints.

## 2 Constraints

In this section, we summarize the constraints that we apply in this study. In particular, we consider constraints from the LHC and other accelerators, as derived from searches for mono- $X$  events with missing energy (where  $X$  denotes a jet, photon, or  $Z$ ), di-jet resonances, di-lepton resonances, exotic Higgs decays, sbottom searches, and exotic upilon decays [70–80]. We also summarize the current status of direct searches for dark matter, including the recent constraints presented by the LUX [68] and PandaX-II [69] Collaborations.

### 2.1 LHC

Searches at CMS and ATLAS provide some of the most stringent constraints on dark matter, as well as on the particles that mediate the interactions of dark matter. In this study, we consider the bounds from the LHC as applied to a wide range of simplified models, the most stringent of which arise from CMS searches for mono-jet+MET, di-jet resonances, di-lepton resonances, di-tau resonances, and sbottom searches. Although we also considered constraints from the ATLAS Collaboration, they were slightly less restrictive than those from CMS.

LHC limits are typically published in one of two ways: (1) assuming a particular model and choice of couplings, a limit is presented on the parameter space in the dark matter mass-mediator mass plane, or (2) a limit is presented on the product of the production cross section and the branching fraction for a particular process. In this study, we will present our results in terms of the mediator mass and the product of the dark matter-mediator and SM-mediator couplings. Thus applying limits from the LHC generally requires translating these bounds into the parameter space under consideration. To calculate the relevant production cross sections and branching ratios, models are built using FeynRules [81] and subsequently imported into MadGraph5\_aMC@NLO [82, 83]. When necessary, we implement PYTHIA 8 [84] to hadronize the final state particles and DELPHES [85] to simulate the detector response. As appropriate, we apply the published cuts on MET, final state momentum, and final state rapidity in our calculations. Throughout this study, we calculate and present all LHC constraints at the 95% confidence level.

In scenarios with heavy mediators, it is not uncommon for the width of the mediator to be unacceptably large (i.e. as large or larger than its mass). Such widths are clearly not physical and may indicate the presence of additional particles or interactions [86–90]. Imposing unitarity and gauge invariance often restricts the mass of such additional particles to be of the same order of magnitude as the other dark sector particles, making it difficult to define the properties of these new particles such that they are beyond the reach of the LHC. Although the construction of more complicated dark sectors is beyond the scope of the work, we emphasize that it is likely that constraints derived on such models would be more restrictive than those derived here. Throughout this study, in order to maintain the

validity of the theory in this region of parameter space, we apply LHC constraints assuming  $\Gamma/m = 0.1$  whenever the width of the mediator would otherwise exceed this value.

## 2.2 LEP-II

Constraints from LEP-II on Higgs bosons in the mass range between 10 GeV and 100 GeV are extremely constraining for a wide range of beyond the SM physics scenarios. In this study we consider such limits as derived from searches for a light Higgs decaying to  $b\bar{b}$  [79]. Although powerful, these constraints are rather model dependent, and generally rely on the scalar mediator’s coupling to the SM gauge bosons. LEP-II constraints are presented at the 95% confidence level throughout this work, and assume a coupling to the Z-boson identical to that of the SM Higgs.

## 2.3 BaBar

We also consider in this study constraints derived from BaBar on upsilon decays to light scalar or pseudoscalar particles, in particular focusing on channels where the mediator subsequently decays to hadrons, muons, taus or charm quarks [91–94]. We consider relativistic and QCD corrections for the decay of a vector meson as described in Ref. [80]. We note that the  $\mu^+\mu^-$  channel provides the strongest constraints, but the precise values of the branching ratios of such light scalars are not well known (see e.g. Refs. [80, 95]). Here, we conservatively assume a 100% branching ratio to hadrons in the mass range of  $1\text{ GeV} \lesssim m_A \lesssim 2m_\tau$ . This is conservative in the sense that introducing a small branching ratio to muons strengthens the resulting bound. For  $2m_\tau \lesssim m_A < 9\text{ GeV}$ , we use the branching ratios as recently computed in Ref. [96] which incorporate QCD corrections. We find similar constraints as those previously obtained in the recent analysis of Refs. [80] and [95] for pseudoscalar and scalar mediators, respectively. All BaBar constraints are presented at the 90% confidence level in this study.

## 2.4 Direct Detection

The constraints utilized in this study on the dark matter’s elastic scattering cross section with nuclei have been derived from the latest results of the LUX Collaboration [68], which are only slightly more stringent than those recently presented by the PANDA-X experiment [69].

For all tree-level cross sections, we use the expressions as presented in Appendices B and C of Ref. [49]. One-loop cross sections for the scalar mediated  $t$ -channel interaction and the  $s$ -channel vector mediated loop-suppressed interaction are provided in Refs. [54] and [97], respectively. The remaining  $t$ -channel models, which are also loop suppressed, suffer from the problem that they are not generically gauge invariant. Consequently, scattering cross sections for these models are calculated by introducing a factor that suppresses the cross section by the same factor that would appear if the interaction were mediated by a massive photon, i.e.  $(g^2 \log(m_b^2/m_{\text{med}}^2)/(64\pi^2 m_{\text{med}}^2))^2$ .

For each model, we calculate the expected number of events in a xenon target following the procedure outlined in Ref. [98], adopting a standard Maxwellian velocity distribution ( $v_0 = 220\text{ km/s}$ ,  $v_{\text{esc}} = 544\text{ km/s}$ ,  $\bar{v}_{\text{Earth}} = 245\text{ km/s}$ ), a local density of  $0.3\text{ GeV/cm}^3$  and an exposure of  $3.35 \times 10^4\text{ kg-day}$ . Form factors and nuclear responses are calculated following the procedures outlined in Refs. [99, 100]. We take the efficiency for nuclear recoils as a function of energy from Fig. 2 of Ref. [68], and derive bounds at the 90% confidence level, assuming 4.2 expected background events and applying Poisson statistics.

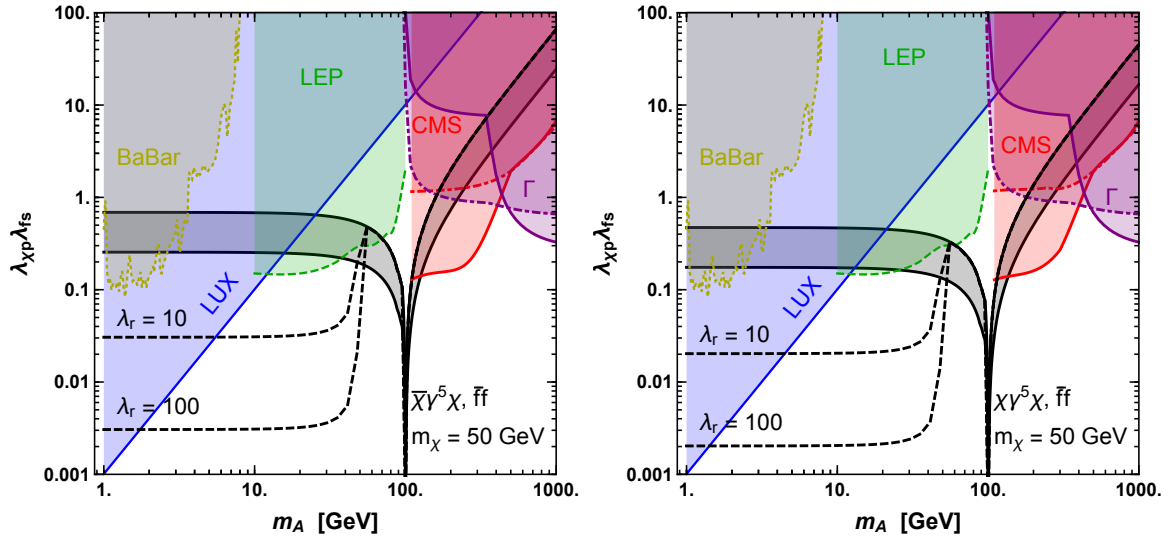


**Figure 1.** Constraints on a 50 GeV Dirac (left) and Majorana (right) dark matter candidate which annihilates through a spin-0 mediator with a pseudoscalar coupling to the dark matter and a (universal) scalar coupling to SM fermions. The black dashed (solid) lines include (neglect) annihilations to mediator pairs for several values of  $\lambda_r \equiv \lambda_\chi/\lambda_b$ . The upper boundary of the shaded black region is where the correct thermal relic abundance is obtained, whereas along the lower boundary the low-velocity annihilation cross section is at its minimum value required to potentially generate the observed gamma-ray excess. The constraints from CMS assume  $\lambda_r = 1/3$  (solid) and  $\lambda_r = 3$  (dash-dot), and are compared with the bounds enforcing  $\Gamma_A/m_A = 0.1$  (purple) for the same coupling ratios. LEP and BaBar constraints are presented for  $\lambda_r = 10$  and 1, respectively.

### 3 Pseudoscalar Mediated Dark Matter

In this section, we will consider models in which the dark matter annihilates through the  $s$ -channel exchange of a spin-0 mediator,  $A$ . We begin by considering a fermionic dark matter candidate,  $\chi$ , with interactions as described by the following Lagrangian:

$$\mathcal{L} \supset \left[ a \bar{\chi} \lambda_{\chi p} i \gamma^5 \chi + \sum_f y_f \bar{f} (\lambda_{fs} + \lambda_{fp} i \gamma^5) f \right] A, \quad (3.1)$$

where  $a = 1(1/2)$  for a Dirac (Majorana) dark matter candidate. Although we describe the interactions of the SM fermions in terms of their yukawas,  $y_f \equiv \sqrt{2}m_f/v$ , the quantities  $\lambda_{fs}$  and  $\lambda_{fp}$  allow for arbitrary values of each coupling. Here,  $v$  is the SM Higgs vacuum expectation value, i.e.  $v \simeq 246$  GeV. Assuming that  $\lambda_{bs}$  or  $\lambda_{bp}$  is not much smaller than that of the other SM fermions, dark matter will annihilate largely to  $b\bar{b}$  in this model. For this dominant annihilation channel, a dark matter mass of approximately 50 GeV is required to generate the observed spectral shape of the Galactic Center excess [17, 101], and we adopt this value throughout this section.

In the left (right) frame of Fig. 1, we plot the constraints on the parameter space of a simplified model with dark matter in the form of a Dirac (Majorana) fermion and a mediator with a pseudoscalar coupling to the dark matter ( $\bar{\chi}\gamma^5\chi$ ) and scalar couplings to SM fermions ( $\bar{f}f$ ), assuming a common scalar coupling to all SM fermions (as motivated

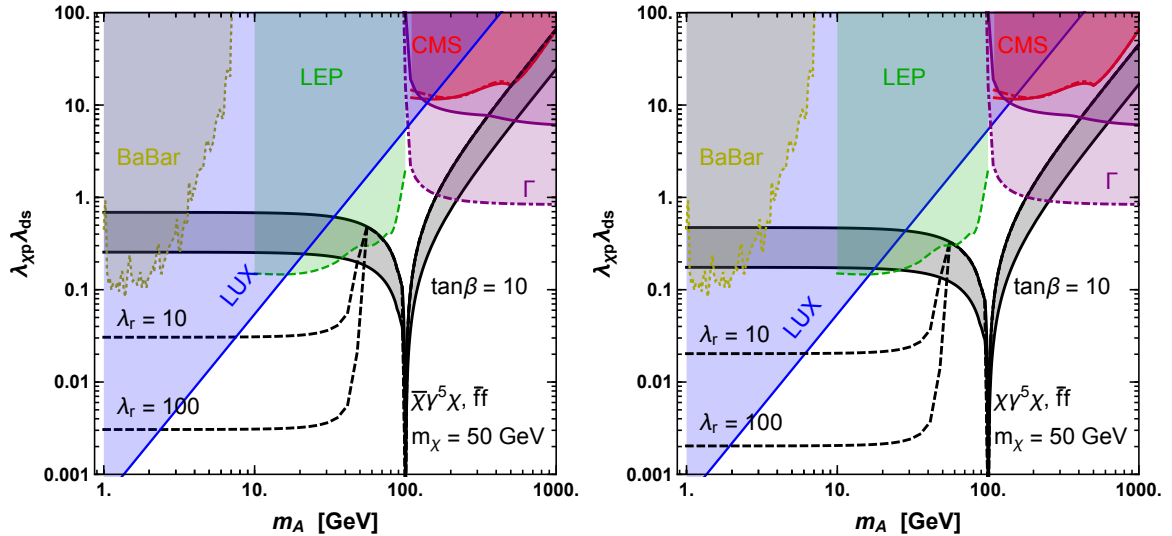


**Figure 2.** As in Fig. 1 but for  $\tan\beta = 10$ , where  $\tan\beta$  is defined as the ratio of the mediator’s couplings to down-type and up-type fermions.

by minimal flavor violation),  $\lambda_{fs}$ <sup>1</sup>. In each frame, the upper boundary of the shaded black region represents the the value of the product of the couplings that is required to generate an acceptable thermal relic abundance, assuming standard cosmology. The lower boundary of this region corresponds to a more relaxed assumption, requiring only that the low-velocity annihilation cross section is large enough to potentially generate the observed gamma-ray excess,  $\langle\sigma_{xx}v\rangle > 3 \times 10^{-27} \text{ cm}^3/\text{s}$  (or twice this value in the case of a Dirac particle). If  $m_A < m_\chi$ , dark matter can annihilate directly to mediator pairs via t-channel  $\chi$  exchange. In these figures, we plot as dashed black lines the parameter space which generates the observed thermal relic abundance for several values of  $\lambda_r \equiv \lambda_\chi/\lambda_b$ . One should keep in mind that if the dark matter annihilates significantly to mediator pairs in the low-velocity limit, a higher value for the dark matter mass is generally required in order for the resulting gamma-ray spectrum to be consistent with the observed features of the Galactic Center excess [53, 62, 63]. We compare these curves to the constraints derived from LUX (blue), CMS/LHC (red), LEP (green), and BaBar (yellow).

In the case of CMS, the most stringent constraint in this class of models derives from searches for events with a single jet and missing transverse energy (MET). As the sensitivity of collider searches depends not only on the product of the couplings, but also on their ratio, we present constraints for multiple values of  $\lambda_r$ . In Fig. 1, the solid (dot-dashed) lines correspond to CMS constraints for  $\lambda_r = 1/3$  (3), while LEP and BaBar constraints are derived assuming  $\lambda_r = 10$  and  $\lambda_r = 1$ , respectively. The regions bounded by a purple solid (dot-dashed) line represent those in which the calculated width of the mediator exceeds one tenth of its mass, for  $\lambda_r = 1/3$  (3). As described in Sec. 2.1, we set  $\Gamma_A = 0.1 m_A$  throughout this region of parameter space, and take this to be indicative of additional particles and/or interactions that are not described by our simplified model.

The constraints from LEP rely on an effective coupling of the SM  $Z$  to  $ZA$ , and are

<sup>1</sup>Note that the product of couplings in these models be quite large, occasionally appearing to violate perturbativity. This need not be the case, however, as we have not included the yukawa contribution to the SM coupling, which may significantly suppress this product.



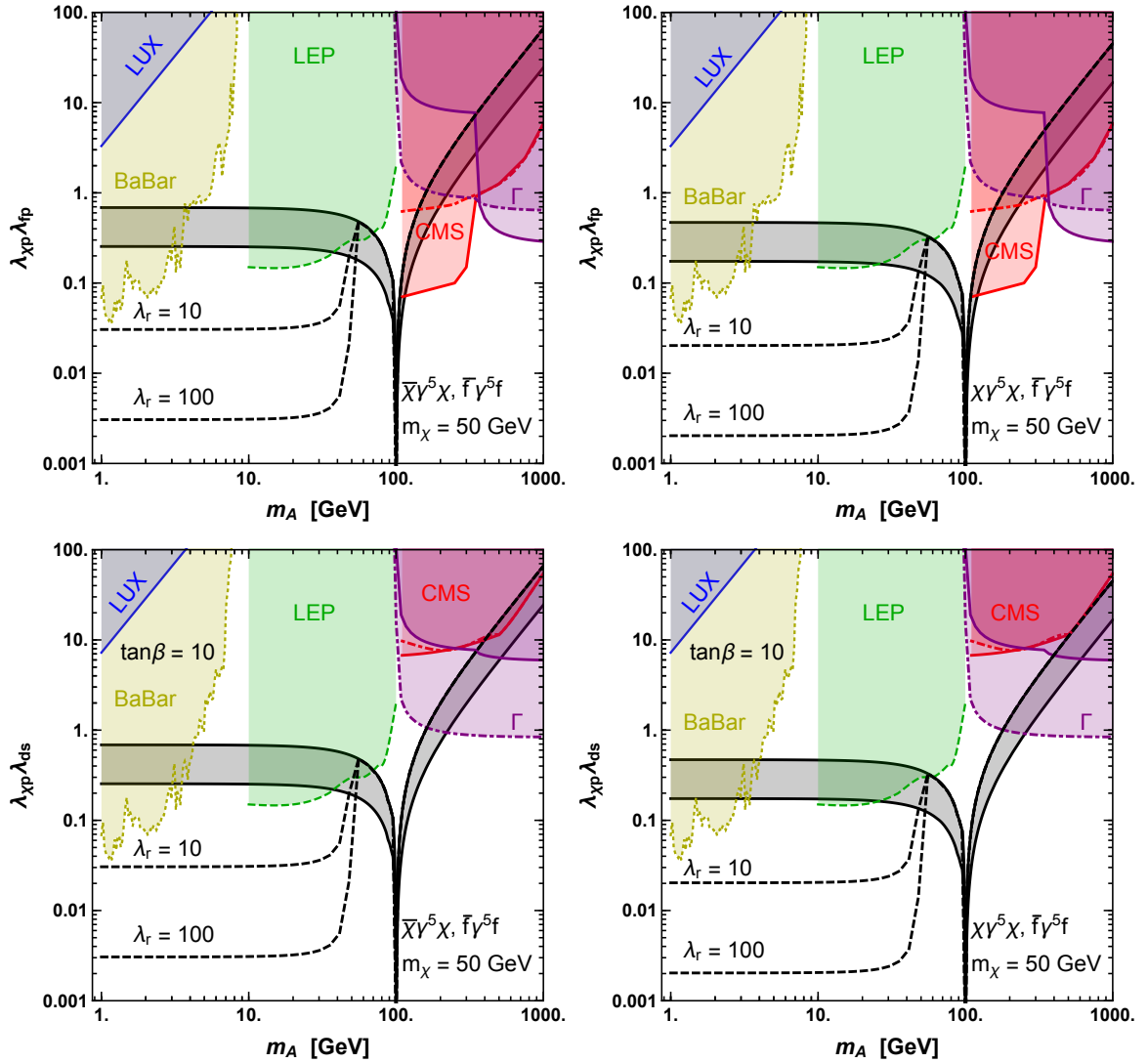


**Figure 3.** As in Fig. 1 but for a mediator with purely pseudoscalar couplings. The upper (lower) frames correspond to  $\tan\beta = 1$  (10).

thus highly model dependent. While this constraint does apply, for example, to the case in which the couplings of the  $A$  to SM fermions are the result of mixing with the SM Higgs, there are many other scenarios in which a spin-0 mediator can couple to the SM fermions while having a suppressed coupling to the  $Z$ .

Several of the constraints shown in Fig. 1 depend on the ratios of the various couplings of the mediator. In particular, since the LHC constraints are dominated by diagrams in which a scalar mediator is produced through a top quark loop, such constraints may be much weaker if the top quark coupling is suppressed. To illustrate this, we plot in Fig. 2 the derived constraints assuming  $\tan\beta = 10$ , where  $\tan\beta$  is defined as the ratio of the mediator's couplings to down-type and up-type fermions,  $\tan\beta \equiv \lambda_d/\lambda_u$ . While bounds from LEP, LUX and BaBar are not significantly affected by the value of  $\tan\beta$ , mono-jet+MET bounds can be noticeably reduced, in particular in the case of  $\lambda_r \ll 1$ . Increasing  $\tan\beta$  also reduces the width of the mediator for  $m_A > 2m_t$ , potentially opening up additional parameter space.



We repeat this exercise in Fig. 3 for the case of a mediator with pseudoscalar couplings to both the dark matter and to SM fermions. In this case, the dark matter’s elastic scattering cross section with nuclei is both spin-dependent and heavily momentum suppressed ( $\sigma_{SD} \propto q^4$ ), making direct detection experiments largely insensitive to these models. The bounds derived from colliders, however, are relatively insensitive to whether SM fermions couple via a scalar or pseudoscalar interaction. We emphasize that, as in the previous case, a large portion of parameter space remains viable for this model, especially should the top-mediator coupling be suppressed.

Next, we consider dark matter in the form of a scalar  $\phi$ , with a Lagrangian given by:

$$\mathcal{L} \supset \left[ a\mu_\phi |\phi|^2 + \sum_f y_f \bar{f} \lambda_{fp} i \gamma^5 f \right] A, \quad (3.2)$$

where  $a = 1(1/2)$  for a complex (real) dark matter particle.

The phenomenology of this model is summarized in Fig. 4, for the cases of a complex (left frame) or real (right frame) scalar. LHC signatures for this model are rather different from in the case of fermionic dark matter as the decay of the spin-0 mediator to dark matter is heavily suppressed. Instead, the dominant constraint from the LHC results from searches for a Higgs-like particle decaying to  $\tau^+\tau^-$ . At very large mediator masses, however, ( $m_A \gtrsim 600$  GeV), the branching ratio to  $\tau^+\tau^-$  is reduced and di-jet resonances become slightly more constraining (this accounts for the dip-like feature appearing in the CMS bound). As in the previous scenarios, LEP bounds on scalar decays to  $b\bar{b}$  are very constraining in the region  $10 \text{ GeV} < m_A < 100 \text{ GeV}$ , but only apply in models in which the mediator couples either directly or indirectly to the  $Z$ .

In the lower frames of Fig. 4, we show how these bounds change if the mediator does not couple to leptons and has an asymmetric coupling to up-like and down-like quarks with  $\tan\beta = 2$ . This choice can open a window of parameter space for  $100 \text{ GeV} \lesssim m_A \lesssim 2m_t$ , depending on the precise values of  $\tan\beta$  and  $\lambda_r$ .

Next, we consider the case of vector dark matter  $X^\mu$ :

$$\mathcal{L} \supset \left[ a\mu_X X^\mu X_\mu^\dagger + \sum_f y_f \bar{f} \lambda_{fp} i \gamma^5 f \right] A, \quad (3.3)$$

where  $a = 1(1/2)$  for a complex (real) dark matter particle.

Constraints on this model are shown in Fig. 5. The dominant decay mode of the mediator in this model, and thus the most constraining LHC search, depends on the mass of the mediator. For  $m_A \simeq 100$  GeV the dominant decay is to dark matter, and thus the most constraining search is that based on mono-jet+MET events. This picture is very different for larger mediator masses, however, for which constraints based on searches for Higgs bosons decaying to  $\tau^+\tau^-$  become more stringent. Both of these search channels significantly exclude mediator masses above 100 GeV in this class of models, for both  $\lambda_r = 3$  and  $\lambda_r = 1/3$ . Similar to in the scalar dark matter case, however, we can relax some of these constraints by suppressing the mediator’s couplings to leptons and/or by increasing  $\tan\beta$  (as shown in the lower frames of Fig. 5).

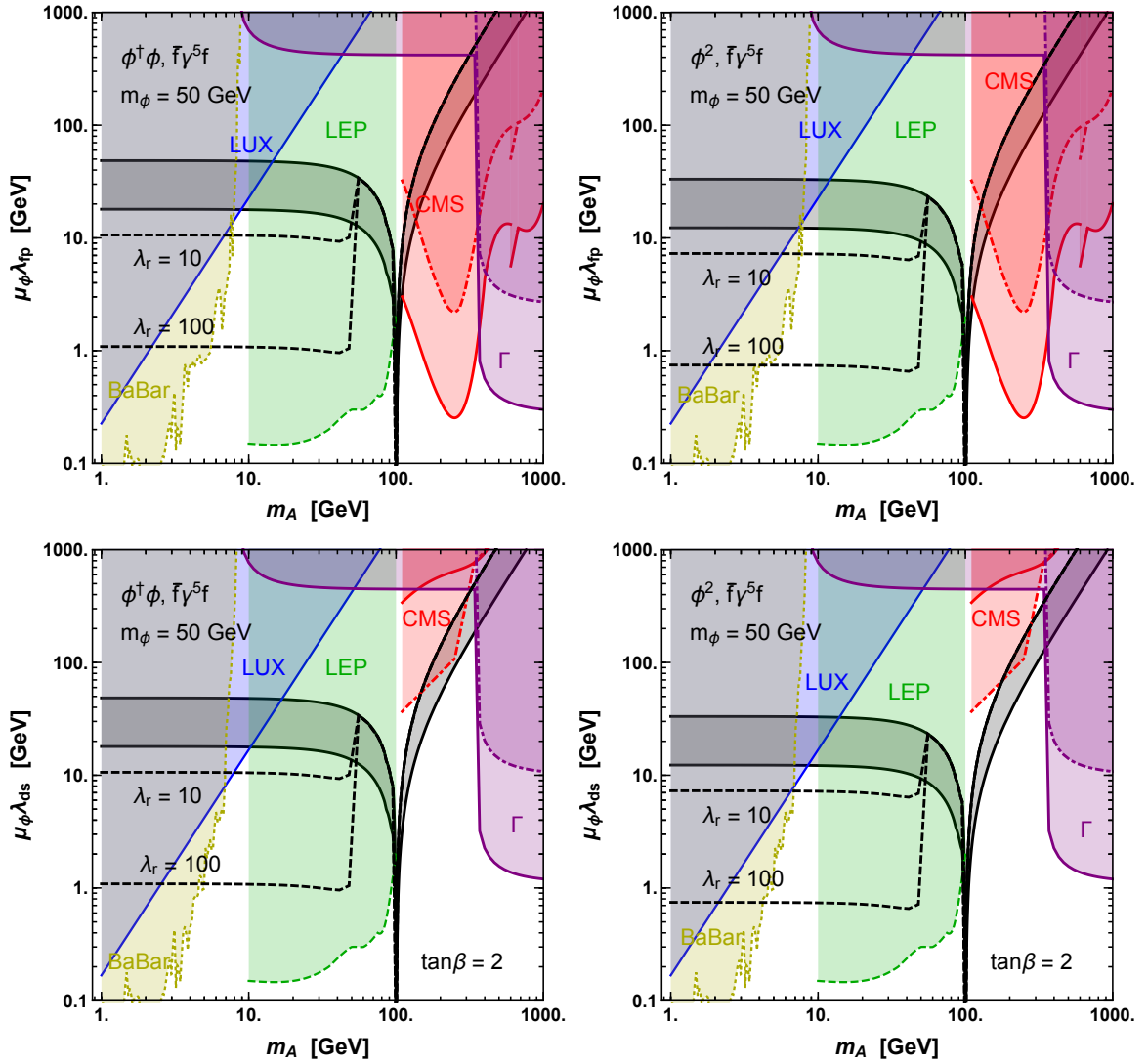


**Figure 4.** As in the previous figures, but for a 50 GeV complex (left) or real (right) scalar dark matter candidate, which annihilates through a spin-0 mediator with a pseudoscalar coupling to SM fermions. In the upper frames, we take the mediator’s couplings to be equal for all SM fermions, whereas in the lower frames the mediator does not couple to leptons and  $\tan\beta = 2$ .

#### 4 Vector Mediated Dark Matter

In this section we consider fermionic dark matter annihilating through the  $s$ -channel exchange of a spin-1 mediator,  $V_\mu$ , with Lagrangians of the form [49, 52]:

$$\mathcal{L} \supset \left[ a\bar{\chi}\gamma^\mu(g_{\chi v} + g_{\chi a}\gamma^5)\chi + \sum_f \bar{f}\gamma^\mu(g_{fv} + g_{fa}\gamma^5)f \right] V_\mu, \quad (4.1)$$

where  $a = 1(1/2)$  for a Dirac (Majorana) dark matter candidate. For the case of comparable couplings to various SM fermions this class of models require a  $\simeq 35$  GeV dark matter candidate to generate a signal consistent with the Galactic Center excess. Unless stated otherwise, we will adopt this value for the dark matter mass throughout this section.

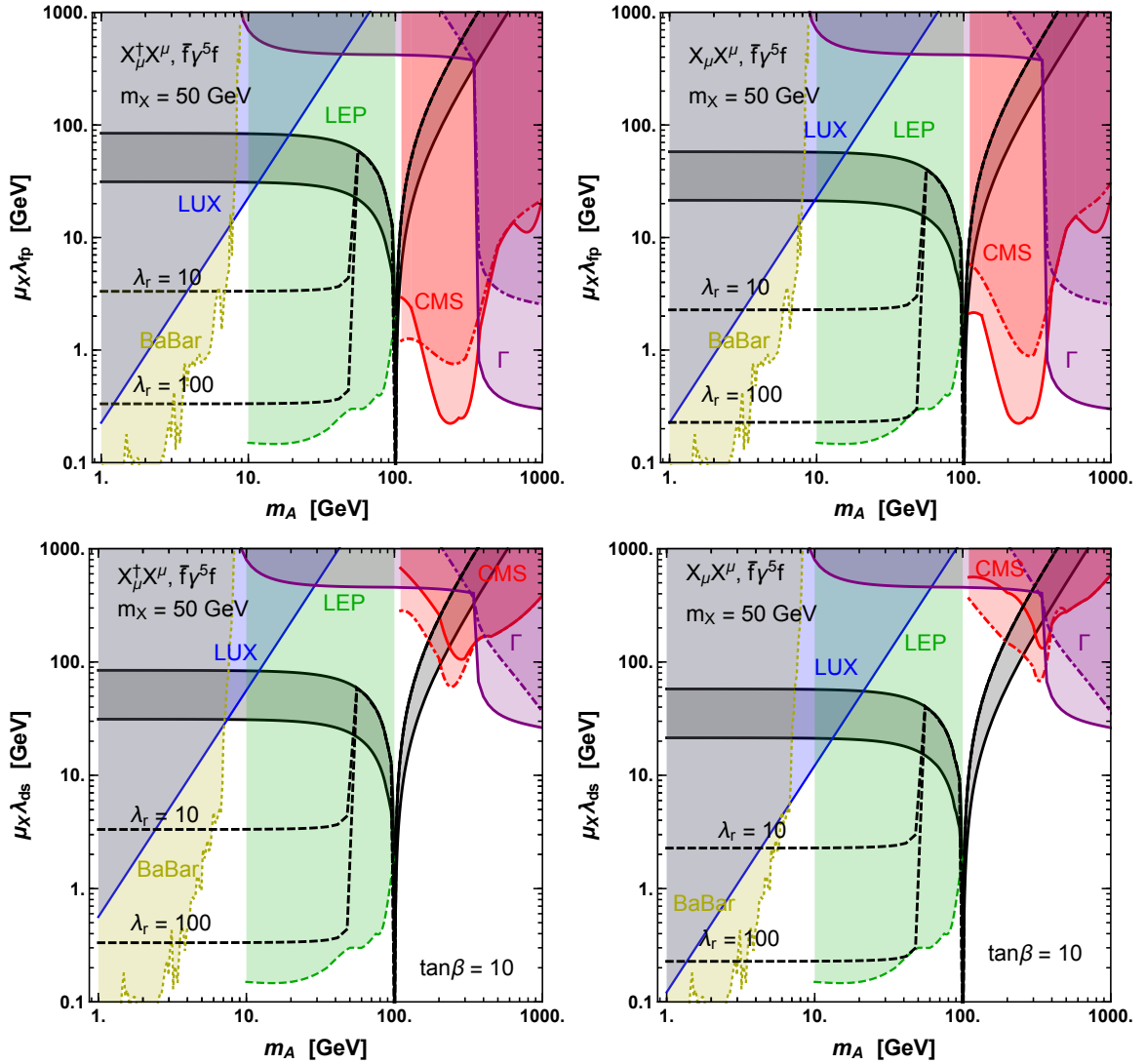


**Figure 5.** As in previous figures, but for a 50 GeV complex (left) and real (right) vector dark matter candidate which annihilates through a spin-0 mediator with a pseudoscalar coupling to SM fermions. In the upper frames, we take the mediator’s couplings to be equal for all SM fermions, whereas in the lower frames the mediator does not couple to leptons and  $\tan\beta = 10$ .

We begin in Fig. 6 by considering the constraints on a Dirac (left) and Majorana (right) dark matter candidate that annihilates through a mediator with purely axial couplings. As spin-dependent elastic scattering with nuclei is unsuppressed in this class of models<sup>2</sup>, current LUX constraints force such models to either live on resonance ( $m_\chi \simeq m_V/2$ ), or have a mediator mass  $m_V < m_\chi$  and with  $\lambda_r \gg 1$ . LHC constraints on this model from searches for di-lepton resonances ( $m_V > 400$  GeV) and mono-jet+MET searches ( $100$  GeV  $< m_V < 400$  GeV) limit mediator masses in this model to be below  $\simeq 100$  GeV. LHC bounds are shown in this figure for  $\lambda_r = 1/3$  (solid) and  $g_{\chi v} = 1$  (i.e.  $\lambda_r \gg 1$ ) (dotted). Collider constraints for

<sup>2</sup>At the nuclear scale, one would in general expect vector couplings to arise at the one-loop level, leading to stronger direct detection bounds [102]. It may be possible to avoid this in some models, however, and thus we conservatively plot direct detection bounds assuming only axial couplings.

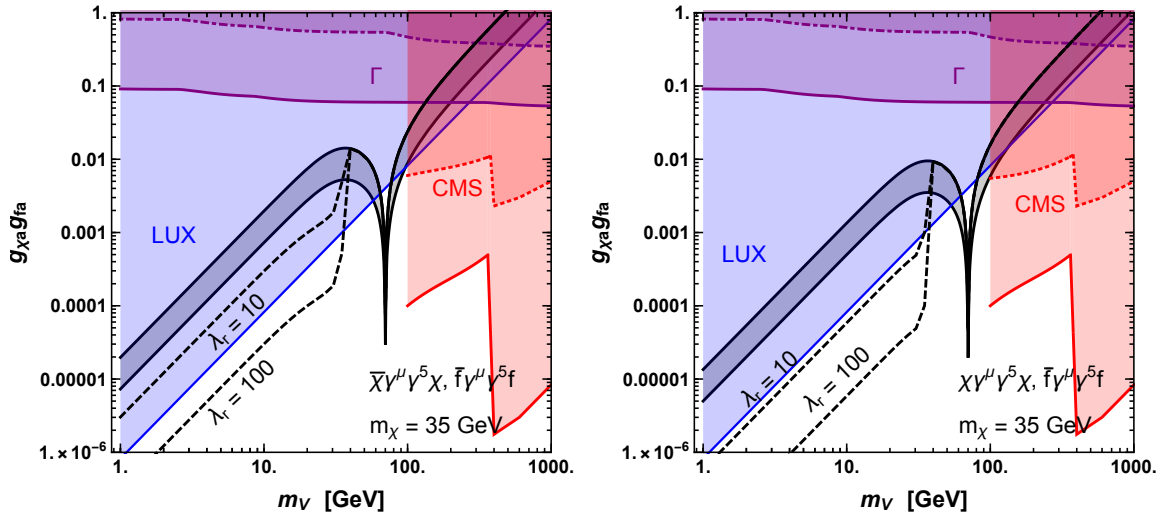


**Figure 6.** As in previous figures, but for a 35 GeV Dirac (left) and Majorana (right) dark matter candidate which annihilates through a spin-1 mediator with axial couplings to both dark matter and (universally) to SM fermions. In this figure, the dotted red (CMS) line corresponds to the case of  $g_{\chi v} = 1$  (i.e.  $\lambda_r \gg 1$ ).

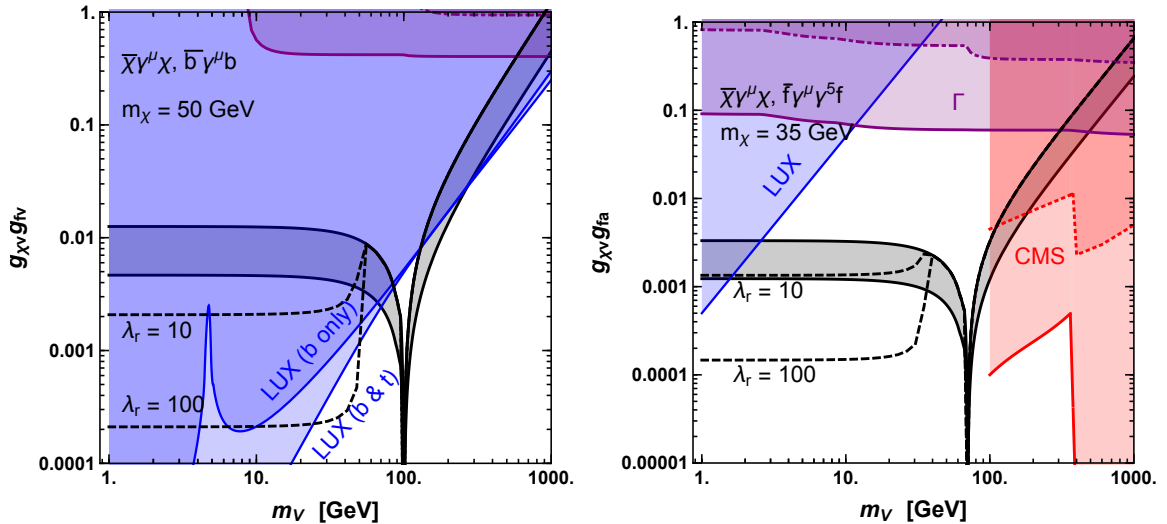


**Figure 7.** As in previous figures, but for a 50 GeV Dirac dark matter candidate with vector couplings to both dark matter and to  $b$ -quarks (left), and for a 35 GeV Dirac dark matter candidate with vector and axial couplings to dark matter and (universally) to SM fermions, respectively (right). LHC bounds are shown for  $\lambda_r = 1/3$  (solid) and  $g_{\chi v} = 1$  (i.e.  $\lambda_r \gg 1$ ) (dotted).

this model are difficult to evade as they do not rely exclusively on couplings to leptons or to specific species of quarks. Such bounds could be evaded, however, if the mediator were to couple exclusively to third generation quarks. An example of such a model is shown in the left frame of Fig. 7, where we consider a 50 GeV Dirac dark matter candidate that annihilates through a spin-1 mediator with vector couplings to both dark matter and  $b$ -quarks (and possibly also  $t$ -quarks). While the leading order elastic scattering diagram arises at loop level in this case, the vector coupling leads to stringent constraints from direct detection

experiments. The dominant constraints from the LHC on vector mediated models typically arise from searches for mono-jet+MET events and di-lepton resonances. Since the production of the vector mediator is in most cases dominated by valence quarks, however, the sensitivity of collider searches is heavily suppressed and thus do not probe significant parameter space in this model. We do not show any LHC constraints in this figure.

In the right panel of Fig. 7, we consider the phenomenology of models where the mediator couples to Dirac dark matter and fermions with a vector and an axial coupling, respectively. The elastic scattering cross section in this case is both spin-dependent and momentum suppressed, and thus such experiments have only recently begun probing this model. LHC constraints from di-lepton resonances ( $m_V > 400$  GeV) and mono-jet+MET searches ( $100 \text{ GeV} < m_V < 400$  GeV) are, as before, extremely constraining. That being said, di-lepton constraints can be easily avoided if the mediator couples only to quarks, and mono-jet constraints can be significantly relaxed if the mediator couples, for example, only to the third generation. LHC bounds are shown for  $\lambda_r = 1/3$  (solid) and  $g_{\chi v} = 1$  (i.e.  $\lambda_r \gg 1$ ) (dotted).

## 5 Dark Matter Annihilating Through $t$ -Channel Mediators

Finally, we consider four scenarios in which the dark matter annihilates through the  $t$ -channel exchange of a colored and electrically charged mediator to  $b\bar{b}$  [54, 103, 104]. These cases consist of a Dirac dark matter candidate,  $\chi$ , and spin-0 mediator,  $A$ :

$$\mathcal{L} \supset \lambda_\chi \bar{\chi}(1 + \gamma^5)fA + \lambda_\chi \bar{f}(1 - \gamma^5)\chi A^\dagger, \quad (5.1)$$

a Dirac dark matter candidate,  $\chi$ , and a spin-1 mediator,  $V_\mu$ :

$$\mathcal{L} \supset g_\chi \bar{\chi}\gamma^\mu(1 + \gamma^5)fV_\mu + g_\chi \bar{f}\gamma^\mu(1 - \gamma^5)\chi V_\mu^\dagger \quad (5.2)$$

and a real or complex vector dark matter candidate,  $X_\mu$ , with a fermionic mediator,  $\psi$ :

$$\mathcal{L} \supset g_X \bar{\psi}\gamma^\mu(1 + \gamma^5)fX_\mu^\dagger + g_X \bar{f}\gamma^\mu(1 - \gamma^5)\psi X_\mu. \quad (5.3)$$

Note that we consider these specific combinations of scalar and pseudoscalar or vector and axial couplings as they are the only examples for which the scalar contact interaction with nuclei is suppressed. Instead, elastic scattering occurs in each of these models through a loop-suppressed vector coupling [49, 54, 105].

In Fig. 8, we summarize the phenomenology of this class of models. In the upper left frame we consider the case of a Dirac dark matter particle and spin-0 mediator. In the remaining frames of this figure, we summarize the phenomenology of models with a Dirac dark matter candidate and a vector mediator (upper right), a complex vector dark matter candidate with a fermionic mediator (lower left), or a real vector dark matter candidate with a fermionic mediator (lower right). In each case, we find that the combination of constraints from the CMS sbottom search and LUX exclude the entire parameter space of this class of models. We also note that the scenarios with a vector dark matter candidate are rather unphysical over much of the parameter space shown due to the very large width of the mediator.

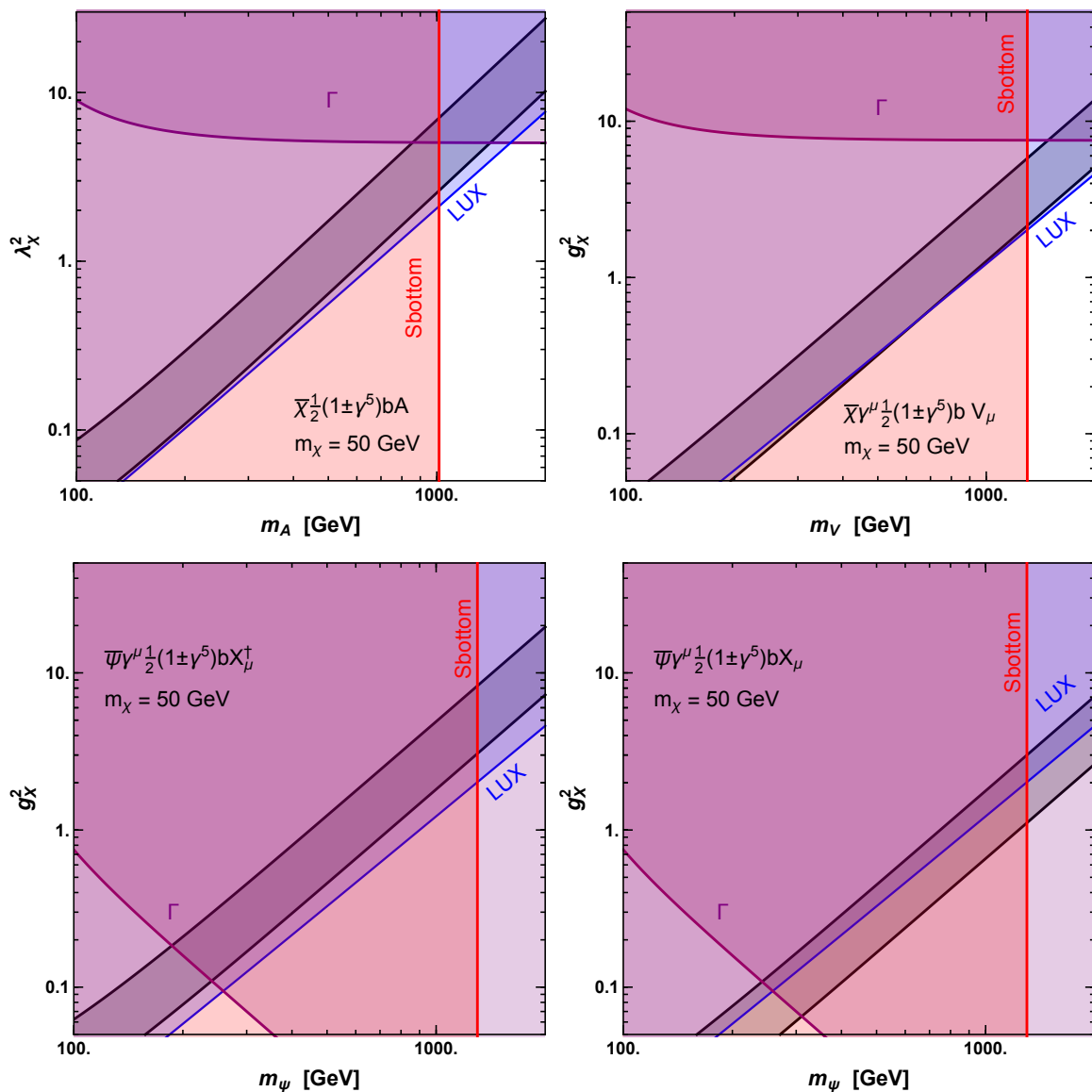


**Figure 8.** As in previous figures, but for a 50 GeV dark matter candidate which annihilates through a  $t$ -channel diagram to  $b\bar{b}$ . In the upper left (right) frame, we consider the case of a Dirac dark matter candidate with a scalar (vector) mediator. In the lower left (right) frame, the dark matter is a real (complex) vector, mediated by a Dirac fermion. The entire parameter space of these models is ruled out by the combined results of LUX and sbottom searches at the LHC.

## 6 Summary and Conclusions

In this study, we have revisited the range of dark matter scenarios that could potentially generate the observed characteristics of the Galactic Center gamma-ray excess, without conflicting with any constraints from colliders or direct detection experiments. We have taken a simplified models approach, considering the 16 scenarios that were previously found to be viable in Ref. [49] (and listed in Table 1). Each of these models features a low-velocity dark matter annihilation cross section that is unsuppressed (i.e.  $s$ -wave), and was found to be

consistent with all constraints as of 2014. Note that we have not considered any hidden sector models (i.e. models in which the dark matter annihilates into unstable particles without sizable couplings to the Standard Model) which, although potentially viable [59, 62, 63], are beyond the scope of this work.

The main results of this study can be summarized as follows:

- Scalar, fermionic, or vector dark matter that annihilates through a mediator with pseudoscalar couplings can in many cases evade all current constraints, for mediator masses between  $\sim 10$  GeV and several hundred GeV.
- Dark matter that annihilates through a spin-1 mediator is ruled out by the results of LUX/PandaX-II unless the mass of the mediator is approximately equal to twice the mass of the dark matter (near an annihilation resonance). An exception to this conclusion is found in the case of a mediator with a purely vector coupling to the dark matter and a purely axial coupling to Standard Model fermions, which is potentially viable for mediator masses between roughly  $\sim 1$  GeV and 200 GeV.
- All scenarios in which the dark matter annihilates through a  $t$ -channel process are now ruled out by a combination of constraints from LUX/PandaX-II and the LHC.
- Constraints from LEP-II and BaBar restrict many of the pseudoscalar mediated scenarios considered in this study. In particular, mediators with a mass in the  $\sim 10$ -100 GeV range are often ruled out by LEP if they couple significantly to the Standard Model  $Z$  (such as in scenarios in which the mediator obtains its couplings to Standard Model fermions through mixing with the Higgs).

Dark matter scenarios that are capable of generating the Galactic Center excess are now significantly more constrained than they were even a few years ago. As the sensitivity of XENON1T, LZ and other direct detection experiments, as well as the LHC, continues to improve, either a discovery will be made, or the vast majority of the currently viable parameter space identified in this study will be excluded. If such searches do advance without the appearance of new signals, hidden sector scenarios will become increasingly attractive, in particular within the context of the Galactic Center.

**Acknowledgments.** We would like to thank Paddy Fox, Roni Harnik, Veronica Sanz, Nuria Rius, and Asher Berlin for helpful discussions. ME is supported by the Spanish FPU13/03111 grant of MEC and also by the European projects H2020-MSCA-RISE-2015 and H2020-MSCA-ITN-2015/674896-ELUSIVES. DH is supported by the US Department of Energy under contract DE-FG02-13ER41958. SW is supported under the University Research Association (URA) Visiting Scholars Award Program, and by a UCLA Dissertation Year Fellowship. Fermilab is operated by Fermi Research Alliance, LLC, under Contract No. DE-AC02-07CH11359 with the US Department of Energy.

## References

- [1] C. Boehm, D. Hooper, J. Silk, M. Casse and J. Paul, *MeV dark matter: Has it been detected?*, *Phys. Rev. Lett.* **92** (2004) 101301, [[astro-ph/0309686](#)].
- [2] D. P. Finkbeiner, *WMAP microwave emission interpreted as dark matter annihilation in the inner galaxy*, [astro-ph/0409027](#).



- [3] D. Hooper, D. P. Finkbeiner and G. Dobler, *Possible evidence for dark matter annihilations from the excess microwave emission around the center of the Galaxy seen by the Wilkinson Microwave Anisotropy Probe*, *Phys. Rev.* **D76** (2007) 083012, [0705.3655].
- [4] PAMELA collaboration, O. Adriani et al., *An anomalous positron abundance in cosmic rays with energies 1.5-100 GeV*, *Nature* **458** (2009) 607–609, [0810.4995].
- [5] AMS collaboration, M. Aguilar et al., *First Result from the Alpha Magnetic Spectrometer on the International Space Station: Precision Measurement of the Positron Fraction in Primary Cosmic Rays of 0.5350 GeV*, *Phys. Rev. Lett.* **110** (2013) 141102.
- [6] C. Weniger, *A Tentative Gamma-Ray Line from Dark Matter Annihilation at the Fermi Large Area Telescope*, *JCAP* **1208** (2012) 007, [1204.2797].
- [7] E. Bulbul, M. Markevitch, A. Foster, R. K. Smith, M. Loewenstein and S. W. Randall, *Detection of An Unidentified Emission Line in the Stacked X-ray spectrum of Galaxy Clusters*, *Astrophys. J.* **789** (2014) 13, [1402.2301].
- [8] A. Boyarsky, O. Ruchayskiy, D. Iakubovskiy and J. Franse, *Unidentified Line in X-Ray Spectra of the Andromeda Galaxy and Perseus Galaxy Cluster*, *Phys. Rev. Lett.* **113** (2014) 251301, [1402.4119].
- [9] FERMI-LAT collaboration, M. Ackermann et al., *Search for gamma-ray spectral lines with the Fermi large area telescope and dark matter implications*, *Phys. Rev.* **D88** (2013) 082002, [1305.5597].
- [10] HITOMI collaboration, F. A. Aharonian et al., *Hitomi constraints on the 3.5 keV line in the Perseus galaxy cluster*, **1607.07420**.
- [11] D. Hooper, P. Blasi and P. D. Serpico, *Pulsars as the Sources of High Energy Cosmic Ray Positrons*, *JCAP* **0901** (2009) 025, [0810.1527].
- [12] I. Cholis and D. Hooper, *Dark Matter and Pulsar Origins of the Rising Cosmic Ray Positron Fraction in Light of New Data From AMS*, *Phys. Rev.* **D88** (2013) 023013, [1304.1840].
- [13] R. M. Crocker et al., *Sub-luminous ‘1991bg-Like’ Thermonuclear Supernovae Account for Most Diffuse Antimatter in the Milky Way*, **1607.03495**.
- [14] M. Su, T. R. Slatyer and D. P. Finkbeiner, *Giant Gamma-ray Bubbles from Fermi-LAT: AGN Activity or Bipolar Galactic Wind?*, *Astrophys. J.* **724** (2010) 1044–1082, [1005.5480].
- [15] FERMI-LAT collaboration, M. Ajello et al., *Fermi-LAT Observations of High-Energy  $\gamma$ -Ray Emission Toward the Galactic Center*, *Astrophys. J.* **819** (2016) 44, [1511.02938].
- [16] T. Daylan, D. P. Finkbeiner, D. Hooper, T. Linden, S. K. N. Portillo, N. L. Rodd et al., *The characterization of the gamma-ray signal from the central Milky Way: A case for annihilating dark matter*, *Phys. Dark Univ.* **12** (2016) 1–23, [1402.6703].
- [17] F. Calore, I. Cholis and C. Weniger, *Background model systematics for the Fermi GeV excess*, *JCAP* **1503** (2015) 038, [1409.0042].
- [18] D. Hooper and T. R. Slatyer, *Two Emission Mechanisms in the Fermi Bubbles: A Possible Signal of Annihilating Dark Matter*, *Phys. Dark Univ.* **2** (2013) 118–138, [1302.6589].
- [19] C. Gordon and O. Macias, *Dark Matter and Pulsar Model Constraints from Galactic Center Fermi-LAT Gamma Ray Observations*, *Phys. Rev.* **D88** (2013) 083521, [1306.5725].
- [20] K. N. Abazajian and M. Kaplinghat, *Detection of a Gamma-Ray Source in the Galactic Center Consistent with Extended Emission from Dark Matter Annihilation and Concentrated Astrophysical Emission*, *Phys. Rev.* **D86** (2012) 083511, [1207.6047].
- [21] D. Hooper and T. Linden, *On The Origin Of The Gamma Rays From The Galactic Center*, *Phys. Rev.* **D84** (2011) 123005, [1110.0006].

- [22] D. Hooper and L. Goodenough, *Dark Matter Annihilation in The Galactic Center As Seen by the Fermi Gamma Ray Space Telescope*, *Phys. Lett.* **B697** (2011) 412–428, [[1010.2752](#)].
- [23] L. Goodenough and D. Hooper, *Possible Evidence For Dark Matter Annihilation In The Inner Milky Way From The Fermi Gamma Ray Space Telescope*, [0910.2998](#).
- [24] B. Zhou, Y.-F. Liang, X. Huang, X. Li, Y.-Z. Fan, L. Feng et al., *GeV excess in the Milky Way: The role of diffuse galactic gamma-ray emission templates*, *Phys. Rev.* **D91** (2015) 123010, [[1406.6948](#)].
- [25] X. Huang, T. Enlin and M. Selig, *Galactic dark matter search via phenomenological astrophysics modeling*, *JCAP* **1604** (2016) 030, [[1511.02621](#)].
- [26] I. Cholis, D. Hooper and T. Linden, *Challenges in Explaining the Galactic Center Gamma-Ray Excess with Millisecond Pulsars*, *JCAP* **1506** (2015) 043, [[1407.5625](#)].
- [27] S. K. Lee, M. Lisanti, B. R. Safdi, T. R. Slatyer and W. Xue, *Evidence for Unresolved  $\gamma$ -Ray Point Sources in the Inner Galaxy*, *Phys. Rev. Lett.* **116** (2016) 051103, [[1506.05124](#)].
- [28] R. Bartels, S. Krishnamurthy and C. Weniger, *Strong support for the millisecond pulsar origin of the Galactic center GeV excess*, *Phys. Rev. Lett.* **116** (2016) 051102, [[1506.05104](#)].
- [29] J. Petrovi, P. D. Serpico and G. Zaharijas, *Millisecond pulsars and the Galactic Center gamma-ray excess: the importance of luminosity function and secondary emission*, *JCAP* **1502** (2015) 023, [[1411.2980](#)].
- [30] D. Hooper, I. Cholis, T. Linden, J. Siegal-Gaskins and T. Slatyer, *Pulsars Cannot Account for the Inner Galaxy's GeV Excess*, *Phys. Rev.* **D88** (2013) 083009, [[1305.0830](#)].
- [31] D. Hooper and G. Mohlabeng, *The Gamma-Ray Luminosity Function of Millisecond Pulsars and Implications for the GeV Excess*, *JCAP* **1603** (2016) 049, [[1512.04966](#)].
- [32] D. Hooper and T. Linden, *The Gamma-Ray Pulsar Population of Globular Clusters: Implications for the GeV Excess*, *JCAP* **1608** (2016) 018, [[1606.09250](#)].
- [33] T. D. Brandt and B. Kocsis, *Disrupted Globular Clusters Can Explain the Galactic Center Gamma Ray Excess*, *Astrophys. J.* **812** (2015) 15, [[1507.05616](#)].
- [34] I. Cholis, C. Evoli, F. Calore, T. Linden, C. Weniger and D. Hooper, *The Galactic Center GeV Excess from a Series of Leptonic Cosmic-Ray Outbursts*, *JCAP* **1512** (2015) 005, [[1506.05119](#)].
- [35] J. Petrovi, P. D. Serpico and G. Zaharija, *Galactic Center gamma-ray "excess" from an active past of the Galactic Centre?*, *JCAP* **1410** (2014) 052, [[1405.7928](#)].
- [36] E. Carlson and S. Profumo, *Cosmic Ray Protons in the Inner Galaxy and the Galactic Center Gamma-Ray Excess*, *Phys. Rev.* **D90** (2014) 023015, [[1405.7685](#)].
- [37] A. Cuoco, M. Krmer and M. Korsmeier, *Novel dark matter constraints from antiprotons in the light of AMS-02*, [1610.03071](#).
- [38] M.-Y. Cui, Q. Yuan, Y.-L. S. Tsai and Y.-Z. Fan, *A possible dark matter annihilation signal in the AMS-02 antiproton data*, [1610.03840](#).
- [39] D. Hooper, T. Linden and P. Mertsch, *What Does The PAMELA Antiproton Spectrum Tell Us About Dark Matter?*, *JCAP* **1503** (2015) 021, [[1410.1527](#)].
- [40] A. Geringer-Sameth, M. G. Walker, S. M. Koushiappas, S. E. Kopusov, V. Belokurov, G. Torrealba et al., *Indication of Gamma-ray Emission from the Newly Discovered Dwarf Galaxy Reticulum II*, *Phys. Rev. Lett.* **115** (2015) 081101, [[1503.02320](#)].
- [41] DES, FERMI-LAT collaboration, A. Drlica-Wagner et al., *Search for Gamma-Ray Emission from DES Dwarf Spheroidal Galaxy Candidates with Fermi-LAT Data*, *Astrophys. J.* **809** (2015) L4, [[1503.02632](#)].

- [42] D. Hooper and T. Linden, *On The Gamma-Ray Emission From Reticulum II and Other Dwarf Galaxies*, *JCAP* **1509** (2015) 016, [[1503.06209](#)].
- [43] S. Li, Y.-F. Liang, K.-K. Duan, Z.-Q. Shen, X. Huang, X. Li et al., *Search for gamma-ray emission from eight dwarf spheroidal galaxy candidates discovered in Year Two of Dark Energy Survey with Fermi-LAT data*, *Phys. Rev.* **D93** (2016) 043518, [[1511.09252](#)].
- [44] DES, FERMI-LAT collaboration, A. Albert et al., *Searching for Dark Matter Annihilation in Recently Discovered Milky Way Satellites with Fermi-LAT*, [1611.03184](#).
- [45] B. Bertoni, D. Hooper and T. Linden, *Is The Gamma-Ray Source 3FGL J2212.5+0703 A Dark Matter Subhalo?*, *JCAP* **1605** (2016) 049, [[1602.07303](#)].
- [46] B. Bertoni, D. Hooper and T. Linden, *Examining The Fermi-LAT Third Source Catalog In Search Of Dark Matter Subhalos*, *JCAP* **1512** (2015) 035, [[1504.02087](#)].
- [47] Z.-Q. Xia et al., *A Spatially-Extended Stable Unidentified GeV Source: 3FGL J1924.8-1034*, [1611.05565](#).
- [48] Y.-P. Wang et al., *Testing the dark matter subhalo hypothesis of the gamma-ray source 3FGL J2212.5+0703*, *Phys. Rev.* **D94** (2016) 123002, [[1611.05135](#)].
- [49] A. Berlin, D. Hooper and S. D. McDermott, *Simplified Dark Matter Models for the Galactic Center Gamma-Ray Excess*, *Phys. Rev.* **D89** (2014) 115022, [[1404.0022](#)].
- [50] S. Ipek, D. McKeen and A. E. Nelson, *A Renormalizable Model for the Galactic Center Gamma Ray Excess from Dark Matter Annihilation*, *Phys. Rev.* **D90** (2014) 055021, [[1404.3716](#)].
- [51] C. Boehm, M. J. Dolan, C. McCabe, M. Spannowsky and C. J. Wallace, *Extended gamma-ray emission from Coy Dark Matter*, *JCAP* **1405** (2014) 009, [[1401.6458](#)].
- [52] D. Hooper, *Z' mediated dark matter models for the Galactic Center gamma-ray excess*, *Phys. Rev.* **D91** (2015) 035025, [[1411.4079](#)].
- [53] A. Berlin, P. Gratia, D. Hooper and S. D. McDermott, *Hidden Sector Dark Matter Models for the Galactic Center Gamma-Ray Excess*, *Phys. Rev.* **D90** (2014) 015032, [[1405.5204](#)].
- [54] P. Agrawal, B. Batell, D. Hooper and T. Lin, *Flavored Dark Matter and the Galactic Center Gamma-Ray Excess*, *Phys. Rev.* **D90** (2014) 063512, [[1404.1373](#)].
- [55] E. Izaguirre, G. Krnjaic and B. Shuve, *The Galactic Center Excess from the Bottom Up*, *Phys. Rev.* **D90** (2014) 055002, [[1404.2018](#)].
- [56] C. Cheung, M. Papucci, D. Sanford, N. R. Shah and K. M. Zurek, *NMSSM Interpretation of the Galactic Center Excess*, *Phys. Rev.* **D90** (2014) 075011, [[1406.6372](#)].
- [57] D. G. Cerdeo, M. Peir and S. Robles, *Low-mass right-handed sneutrino dark matter: SuperCDMS and LUX constraints and the Galactic Centre gamma-ray excess*, *JCAP* **1408** (2014) 005, [[1404.2572](#)].
- [58] A. Alves, S. Profumo, F. S. Queiroz and W. Shepherd, *Effective field theory approach to the Galactic Center gamma-ray excess*, *Phys. Rev.* **D90** (2014) 115003, [[1403.5027](#)].
- [59] D. Hooper, N. Weiner and W. Xue, *Dark Forces and Light Dark Matter*, *Phys. Rev.* **D86** (2012) 056009, [[1206.2929](#)].
- [60] P. Ko, W.-I. Park and Y. Tang, *Higgs portal vector dark matter for GeV scale  $\gamma$ -ray excess from galactic center*, *JCAP* **1409** (2014) 013, [[1404.5257](#)].
- [61] C. Boehm, M. J. Dolan and C. McCabe, *A weighty interpretation of the Galactic Centre excess*, *Phys. Rev.* **D90** (2014) 023531, [[1404.4977](#)].

- [62] M. Abdullah, A. DiFranzo, A. Rajaraman, T. M. P. Tait, P. Tanedo and A. M. Wijangco, *Hidden on-shell mediators for the Galactic Center  $\gamma$ -ray excess*, *Phys. Rev.* **D90** (2014) 035004, [[1404.6528](#)].
- [63] A. Martin, J. Shelton and J. Unwin, *Fitting the Galactic Center Gamma-Ray Excess with Cascade Annihilations*, *Phys. Rev.* **D90** (2014) 103513, [[1405.0272](#)].
- [64] J. M. Cline, G. Dupuis, Z. Liu and W. Xue, *The windows for kinetically mixed  $Z'$ -mediated dark matter and the galactic center gamma ray excess*, *JHEP* **08** (2014) 131, [[1405.7691](#)].
- [65] Y. G. Kim, K. Y. Lee, C. B. Park and S. Shin, *Secluded singlet fermionic dark matter driven by the Fermi gamma-ray excess*, *Phys. Rev.* **D93** (2016) 075023, [[1601.05089](#)].
- [66] C. Karwin, S. Murgia, T. M. P. Tait, T. A. Porter and P. Tanedo, *Dark Matter Interpretation of the Fermi-LAT Observation Toward the Galactic Center*, [1612.05687](#).
- [67] K. Ghorbani, *Fermionic dark matter with pseudo-scalar Yukawa interaction*, *JCAP* **1501** (2015) 015, [[1408.4929](#)].
- [68] D. S. Akerib et al., *Results from a search for dark matter in the complete LUX exposure*, [1608.07648](#).
- [69] PANDAX-II collaboration, A. Tan et al., *Dark Matter Results from First 98.7 Days of Data from the PandaX-II Experiment*, *Phys. Rev. Lett.* **117** (2016) 121303, [[1607.07400](#)].
- [70] CMS collaboration, V. Khachatryan et al., *Search for narrow resonances in dilepton mass spectra in proton-proton collisions at  $\sqrt{s} = 13$  TeV and combination with 8 TeV data*, [1609.05391](#).
- [71] CMS collaboration, V. Khachatryan et al., *Search for narrow resonances decaying to dijets in proton-proton collisions at  $\sqrt{s} = 13$  TeV*, *Phys. Rev. Lett.* **116** (2016) 071801, [[1512.01224](#)].
- [72] CMS collaboration, C. Collaboration, *Search for dark matter in final states with an energetic jet, or a hadronically decaying  $W$  or  $Z$  boson using 12.9 fb $^{-1}$  of data at  $\sqrt{s} = 13$  TeV*, .
- [73] CMS COLLABORATION collaboration, *An inclusive search for new phenomena in final states with one or more jets and missing transverse momentum at 13 TeV with the AlphaT variable*, Tech. Rep. CMS-PAS-SUS-16-016, CERN, Geneva, 2016.
- [74] ATLAS collaboration, T. A. collaboration, *Search for new high-mass resonances in the dilepton final state using proton-proton collisions at  $\sqrt{s} = 13$  TeV with the ATLAS detector*, .
- [75] ATLAS collaboration, M. Aaboud et al., *Search for new phenomena in final states with an energetic jet and large missing transverse momentum in pp collisions at  $\sqrt{s} = 13$  TeV using the ATLAS detector*, *Phys. Rev.* **D94** (2016) 032005, [[1604.07773](#)].
- [76] ATLAS collaboration, M. Aaboud et al., *Search for new phenomena in events with a photon and missing transverse momentum in pp collisions at  $\sqrt{s} = 13$  TeV with the ATLAS detector*, *JHEP* **06** (2016) 059, [[1604.01306](#)].
- [77] CMS collaboration, C. Collaboration, *Search for a neutral MSSM Higgs boson decaying into  $\tau\tau$  at 13 TeV*, .
- [78] CMS collaboration, C. Collaboration, *Search for a narrow heavy decaying to bottom quark pairs in the 13 TeV data sample*, .
- [79] OPAL, DELPHI, LEP WORKING GROUP FOR HIGGS BOSON SEARCHES, ALEPH, L3 collaboration, R. Barate et al., *Search for the standard model Higgs boson at LEP*, *Phys. Lett.* **B565** (2003) 61–75, [[hep-ex/0306033](#)].
- [80] M. J. Dolan, F. Kahlhoefer, C. McCabe and K. Schmidt-Hoberg, *A taste of dark matter: Flavour constraints on pseudoscalar mediators*, *JHEP* **03** (2015) 171, [[1412.5174](#)].

- [81] A. Alloul, N. D. Christensen, C. Degrande, C. Duhr and B. Fuks, *FeynRules 2.0 - A complete toolbox for tree-level phenomenology*, *Comput. Phys. Commun.* **185** (2014) 2250–2300, [[1310.1921](#)].
- [82] J. Alwall, R. Frederix, S. Frixione, V. Hirschi, F. Maltoni, O. Mattelaer et al., *The automated computation of tree-level and next-to-leading order differential cross sections, and their matching to parton shower simulations*, *JHEP* **07** (2014) 079, [[1405.0301](#)].
- [83] V. Hirschi and O. Mattelaer, *Automated event generation for loop-induced processes*, *JHEP* **10** (2015) 146, [[1507.00020](#)].
- [84] T. Sjostrand, S. Mrenna and P. Z. Skands, *A Brief Introduction to PYTHIA 8.1*, *Comput. Phys. Commun.* **178** (2008) 852–867, [[0710.3820](#)].
- [85] DELPHES 3 collaboration, J. de Favereau, C. Delaere, P. Demin, A. Giammanco, V. Lematre, A. Mertens et al., *DELPHES 3, A modular framework for fast simulation of a generic collider experiment*, *JHEP* **02** (2014) 057, [[1307.6346](#)].
- [86] M. Duerr, F. Kahlhoefer, K. Schmidt-Hoberg, T. Schwetz and S. Vogl, *How to save the WIMP: global analysis of a dark matter model with two s-channel mediators*, *JHEP* **09** (2016) 042, [[1606.07609](#)].
- [87] C. Englert, M. McCullough and M. Spannowsky, *S-Channel Dark Matter Simplified Models and Unitarity*, *Phys. Dark Univ.* **14** (2016) 48–56, [[1604.07975](#)].
- [88] G. Busoni et al., *Recommendations on presenting LHC searches for missing transverse energy signals using simplified s-channel models of dark matter*, [1603.04156](#).
- [89] F. Kahlhoefer, K. Schmidt-Hoberg, T. Schwetz and S. Vogl, *Implications of unitarity and gauge invariance for simplified dark matter models*, *JHEP* **02** (2016) 016, [[1510.02110](#)].
- [90] J. Abdallah et al., *Simplified Models for Dark Matter Searches at the LHC*, *Phys. Dark Univ.* **9-10** (2015) 8–23, [[1506.03116](#)].
- [91] BABAR collaboration, J. P. Lees et al., *Search for hadronic decays of a light Higgs boson in the radiative decay  $\Upsilon \rightarrow \gamma A^0$* , *Phys. Rev. Lett.* **107** (2011) 221803, [[1108.3549](#)].
- [92] BABAR collaboration, J. P. Lees et al., *Search for a low-mass scalar Higgs boson decaying to a tau pair in single-photon decays of  $\Upsilon(1S)$* , *Phys. Rev.* **D88** (2013) 071102, [[1210.5669](#)].
- [93] BABAR collaboration, J. P. Lees et al., *Search for di-muon decays of a low-mass Higgs boson in radiative decays of the  $\Upsilon(1S)$* , *Phys. Rev.* **D87** (2013) 031102, [[1210.0287](#)].
- [94] BABAR collaboration, J. P. Lees et al., *Search for a light Higgs resonance in radiative decays of the  $Y(1S)$  with a charm tag*, *Phys. Rev.* **D91** (2015) 071102, [[1502.06019](#)].
- [95] J. D. Clarke, R. Foot and R. R. Volkas, *Phenomenology of a very light scalar mixing with the SM Higgs*, *JHEP* **02** (2014) 123, [[1310.8042](#)].
- [96] U. Haisch and J. F. Kamenik, *Searching for new spin-0 resonances at LHCb*, *Phys. Rev.* **D93** (2016) 055047, [[1601.05110](#)].
- [97] J. Kopp, V. Niro, T. Schwetz and J. Zupan, *DAMA/LIBRA and leptonically interacting Dark Matter*, *Phys. Rev.* **D80** (2009) 083502, [[0907.3159](#)].
- [98] C. Savage, G. Gelmini, P. Gondolo and K. Freese, *Compatibility of DAMA/LIBRA dark matter detection with other searches*, *JCAP* **0904** (2009) 010, [[0808.3607](#)].
- [99] H.-Y. Cheng and C.-W. Chiang, *Revisiting Scalar and Pseudoscalar Couplings with Nucleons*, *JHEP* **07** (2012) 009, [[1202.1292](#)].
- [100] A. L. Fitzpatrick, W. Haxton, E. Katz, N. Lubbers and Y. Xu, *The Effective Field Theory of Dark Matter Direct Detection*, *JCAP* **1302** (2013) 004, [[1203.3542](#)].



- [101] F. Calore, I. Cholis, C. McCabe and C. Weniger, *A Tale of Tails: Dark Matter Interpretations of the Fermi GeV Excess in Light of Background Model Systematics*, *Phys. Rev.* **D91** (2015) 063003, [[1411.4647](#)].
- [102] F. D’Eramo, B. J. Kavanagh and P. Panci, *You can hide but you have to run: direct detection with vector mediators*, *JHEP* **08** (2016) 111, [[1605.04917](#)].
- [103] B. Batell, T. Lin and L.-T. Wang, *Flavored Dark Matter and R-Parity Violation*, *JHEP* **01** (2014) 075, [[1309.4462](#)].
- [104] P. Agrawal, S. Blanchet, Z. Chacko and C. Kilic, *Flavored Dark Matter, and Its Implications for Direct Detection and Colliders*, *Phys. Rev.* **D86** (2012) 055002, [[1109.3516](#)].
- [105] P. Agrawal, Z. Chacko, C. Kilic and R. K. Mishra, *A Classification of Dark Matter Candidates with Primarily Spin-Dependent Interactions with Matter*, [1003.1912](#).